Fabrication and Characterization of a p-AgO/PSi/n-Si Heterojunction for Solar Cell Applications

Nadir F. Habubi, Ahmed N. Abd, Mohammed O. Dawood & A. H. Reshak

Silicon

ISSN 1876-990X
Volume 10
Number 2

Silicon (2018) 10:371-376
DOI 10.1007/s12633-016-9457-1

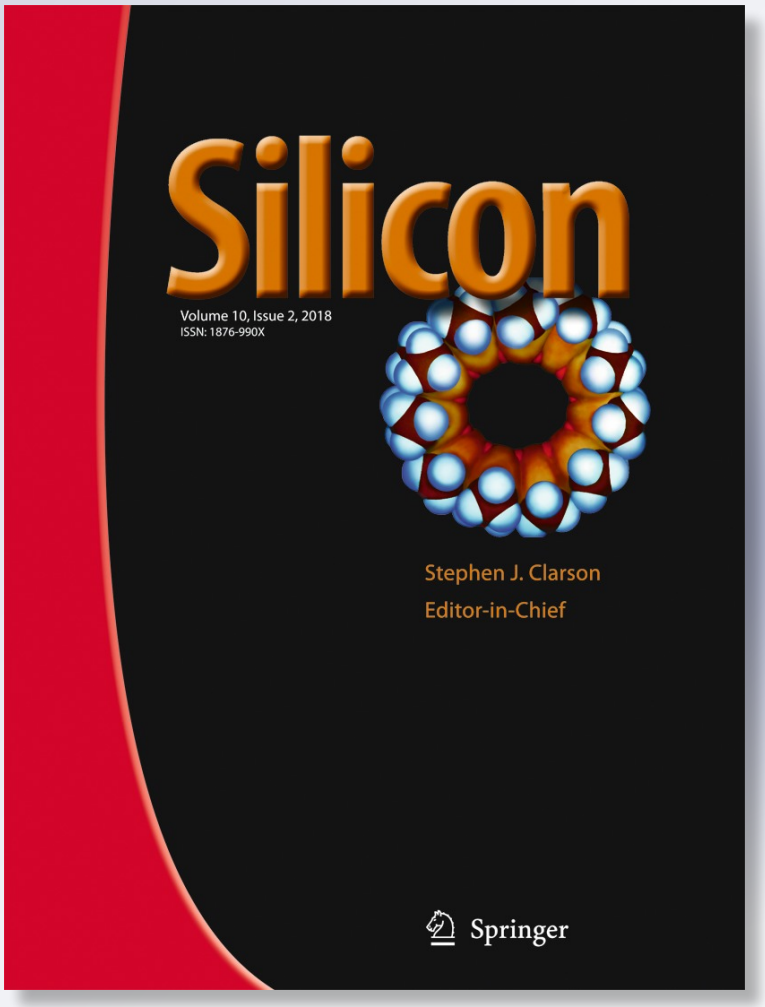

Springer

Silicon (2018) 10:371–376
DOI 10.1007/s12633-016-9457-1

ORIGINAL PAPER

Fabrication and Characterization of a p-AgO/PSi/n-Si Heterojunction for Solar Cell Applications

Nadir F. Habubi[1] · Ahmed N. Abd[2] · Mohammed O. Dawood[2] · A. H. Reshak[3,4]

Received: 21 March 2016 / Accepted: 10 August 2016 / Published online: 15 September 2016

Abstract A p-AgO/PSi/n-Si heterojunction was deposited by high vacuum thermal evaporation of silver subjected to thermal oxidation at 300 °C on porous silicon. Surface morphology and electrical properties of this structure have been studied. The X-ray diffraction (XRD) analysis reveals that the peaks at the (220) and (111) planes were dominated for the crystal quality of the AgO films. The band gap of the AgO films was found to be 2.2 eV and 3.2 eV . The positive sign of Hall effect confirms that the film was of p-type conductivity. The average grain size of pore was measured from the atomic force microscope (AFM) analysis and found to be around 32 nm. The responsivity photodetector after deposited AgO have revealed increasing in response.

Keywords AgO · Thermal oxidation · Lifetime · Heterodiode · XRD · AFM · SEM

✉ Nadir F. Habubi
nadirfadhil@yahoo.com

1 Physics Department, Education Faculty, University of Al- Mustansiriyah, Baghdad, Iraq

2 Physics Department, Science Faculty, University of Al- Mustansiriyah, Baghdad, Iraq

3 New Technologies - Research Centre, University of West Bohemia, Univerzitni 8, 306 14 Pilsen, Czech Republic

4 Center of Excellence Geopolymer and Green Technology, School of Material Engineering, University Malaysia Perlis, 01007 Kangar, Perlis, Malaysia

1 Introduction

Silver oxide (AgO) semiconductor films are known to display p-type semiconductor properties with a bandgap in the range 1.20-3.4 eV [1]. Silver oxides crystallize out by a numerous types of crystal structures, leading to diverse of interesting physiochemical properties such as catalytic, electrochemical, electronic and optical properties [2]. It is known that the AgO phase was relatively steady at high oxygen pressures and at low temperatures. The AgO inhabits different crystal systems such as cubic, monoclinic and tetragonal [3–5]. It is known that the silver, because of its d-shell electrons, exists in different oxidation states and forms several oxides for instance AgO, Ag_2O, Ag_3O, Ag_2O_3. The action of forming of these oxides depends upon the growth conditions/reaction kinetics, accessibility of oxygen in the growth chamber and the energy required for the oxidation. The surface morphology and the nucleation kinetics of the silver oxide rely on the kinetic energy of the particles (silver and oxygen atoms or silver oxide molecules) access to the substrate [6]. Among the various metals, silver showed effective thermal conductivity , high electrical conductivity and can be synthesized into Ag based compounds with different compositions. Silver is more interactive than gold or platinum therefore, silver is the most convenient candidate for various applications [7, 8]. These oxides have variant crystalline structures leading to a different physiochemical, electrochemical, electronic, and optical properties. The most observable and stable phases are Ag_2O and AgO [9]. AgO thin films can be synthesised by using various deposition processes such as thermal oxidation of silver films [10], thermal evaporation [11], electron beam evaporation [12], pulsed laser deposition [13], chemical vapor

deposition [14], electro-deposition [15], DC sputtering [16] and RF sputtering [17].

In the current work, successful fabrication of a p-AgO/PSi/n-Si heterojunction by using electrochemical etching of silicon and deposition of Ag thin films by thermal evaporation and rapid oxidation of the films at 300 °C are reported. The structural and optical characterizations of the AgO/PSi/P-Si heterojunction were performed.

2 Experimental Details

The n-PSi layers were fabricated by anodic etching where a n-type silicon n-Si (1- 4.5) Ω .cm resistivity , of an area (1×1) cm^2 dimensions, 0.785 cm^2 etched area substrate was placed in the teflon etching cell using an admixture of aqueous hydrogen fluoride (purity 47 %) and ethanol (purity 99.99 %), 1:1 by volume. The sample was anodized at a current density of 10 mA/cm^2 and at 15 min etching time. No further chemical or thermal treatment were carried after etching.

High purity (99.99 %) Ag thin film was deposited on the n-PSi substrates by using thermal evaporation system type (Edwards). The pressure deposition 2×10^{-5} mbar and the thickness of films were 200 nm, then Ag thin film was thermally oxidate by using a tube furness homemade at 300 °C for 60 min in static air. The bottom of PSi and above of AgO electrodes was coated with a thick aluminum layer in order to measure the electrical properties. It was obtained under vacuum of Al wire of high purity (99.99 %). The evaporation process was started at a pressure of $5x10^{-6}$ mbar.

Table 1 Summary of XRD characterization

2 θ (°)	(hkl) planes	β(°)	G_s(nm)	η $x10^{-4}$	δ $x10^{14}$ (lines/m^2)
38.26	111 (Ag)	0.15	55.78	6.21	3.217
44.43	200 (Ag)	0.16	50.53	6.85	3.915
64.57	220 (AgO)	0.15	59.25	5.84	2.848
77.51	111 (AgO)	0.17	59.76	5.79	2.800

Structural properties were studied by using X-ray diffractometer type (XRD-6000, SHIMADZU, X-RAY DIFFRACTOMETER) with Cukα radiation of wavelength (λ = 1.54056 Å). Optical absorption of thin film and porous silicon layer were measured using spectrophotometer type(CARY, 100 CONC plus, UV-Vis-NIR, Split- beam Optics, Dual detectors) in the wavelength range of (200-900 nm). The shape and size of AgO were investigated by using SEM and AFM type (AA 3000 Scanning Probe Microscope). The electrical characterization was carried out using Hall measurements after making ohmic contacts through a special mask on the film of AgO deposited on a glass substrate. Thickness of films were measured using ellipsometer (Angestrom sun Technologies Ins). The spectral responsivity of the photodiode was measured in the spectral range (400-1100) nm using a calibrated monochromator.

3 Results and Discussion

Figure 1 shows the XRD pattern of AgO thin film, which contain four main peaks at diffraction angles of 38.26°, 44.43° corresponds to (111), (200) of silver is observed

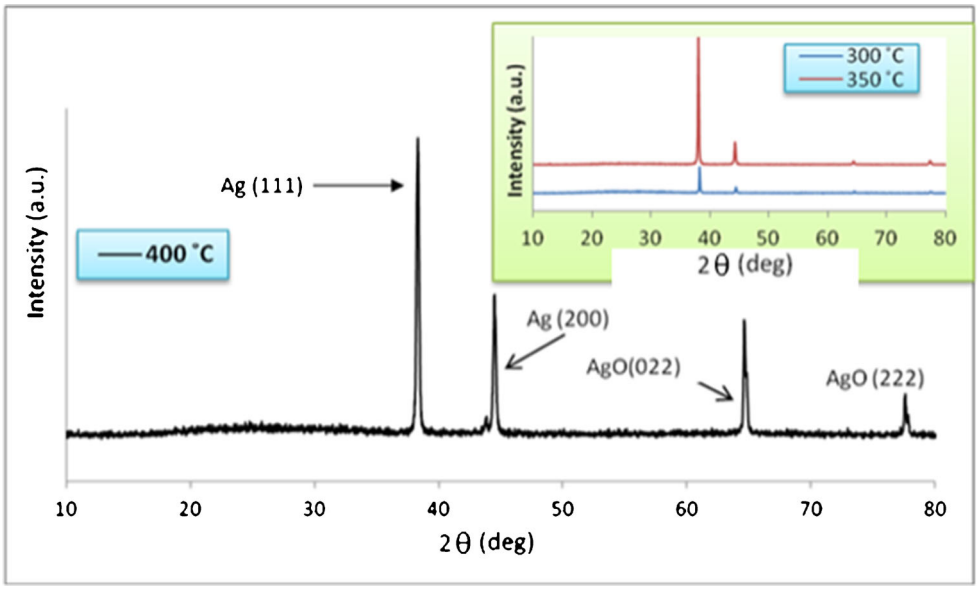

Fig. 1 XRD pattern of AgO thin film at 300 °C oxidation temperature and the inset XRD pattern for Ag thin film at 100 °C and 200 °C oxidation temperature

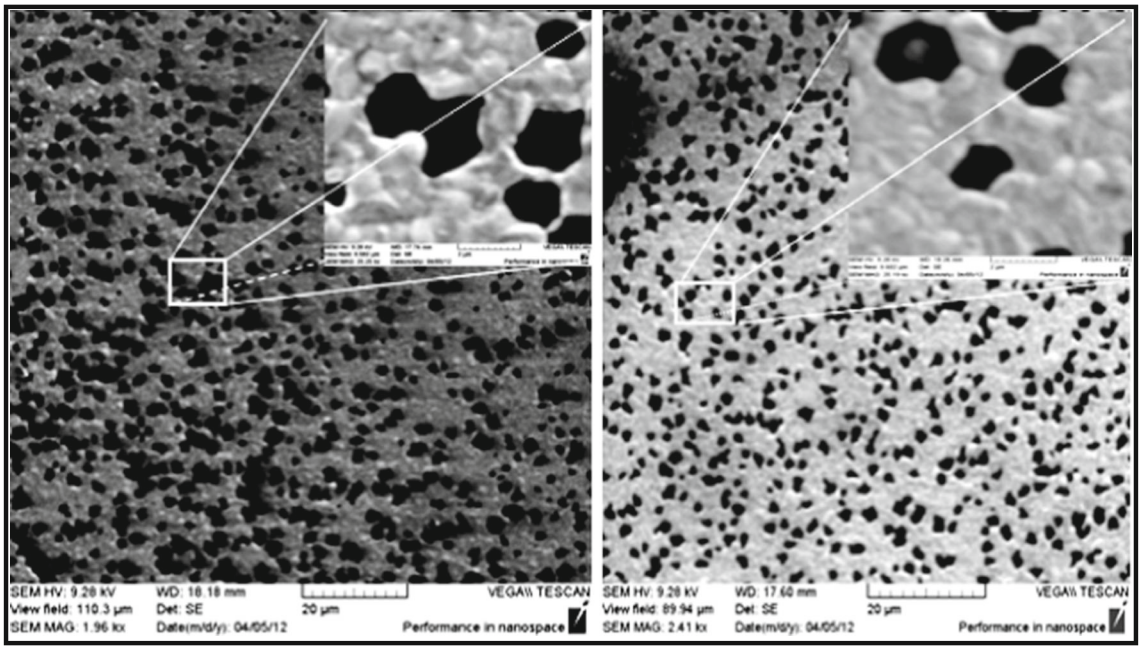

Fig. 2 SEM images of the Ag (*left*) and AgO (*right*) thin films

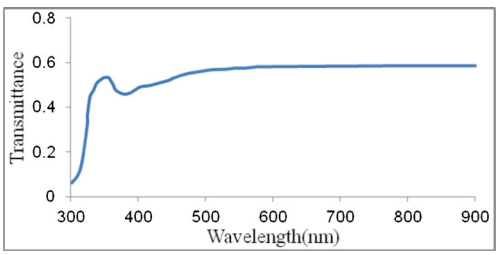

Fig. 3 Optical transmittance of AgO thin film deposited on a glass substrate

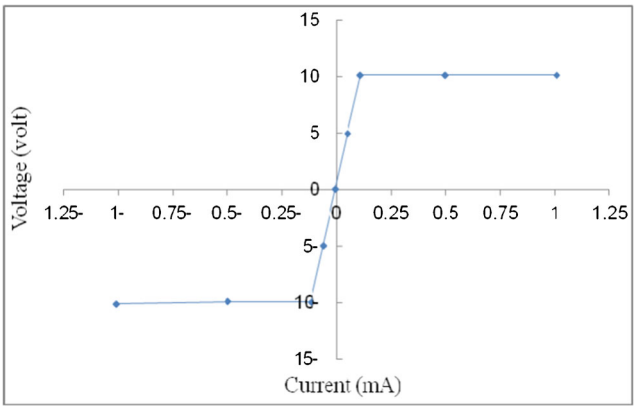

Fig. 5 I-V of AgO thin film deposited on glass

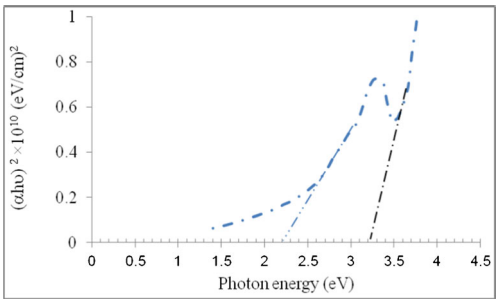

Fig. 4 $(\alpha h\upsilon)^2$ versus $h\upsilon$ for AgO thin films deposited on glass

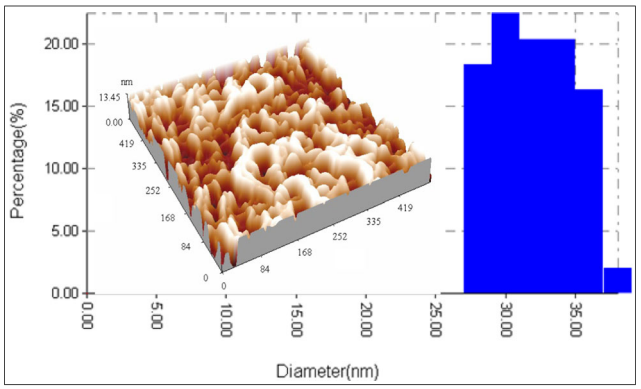

Fig. 6 3-D AFM image of the porous silicon (PSi) layer and chart distribution

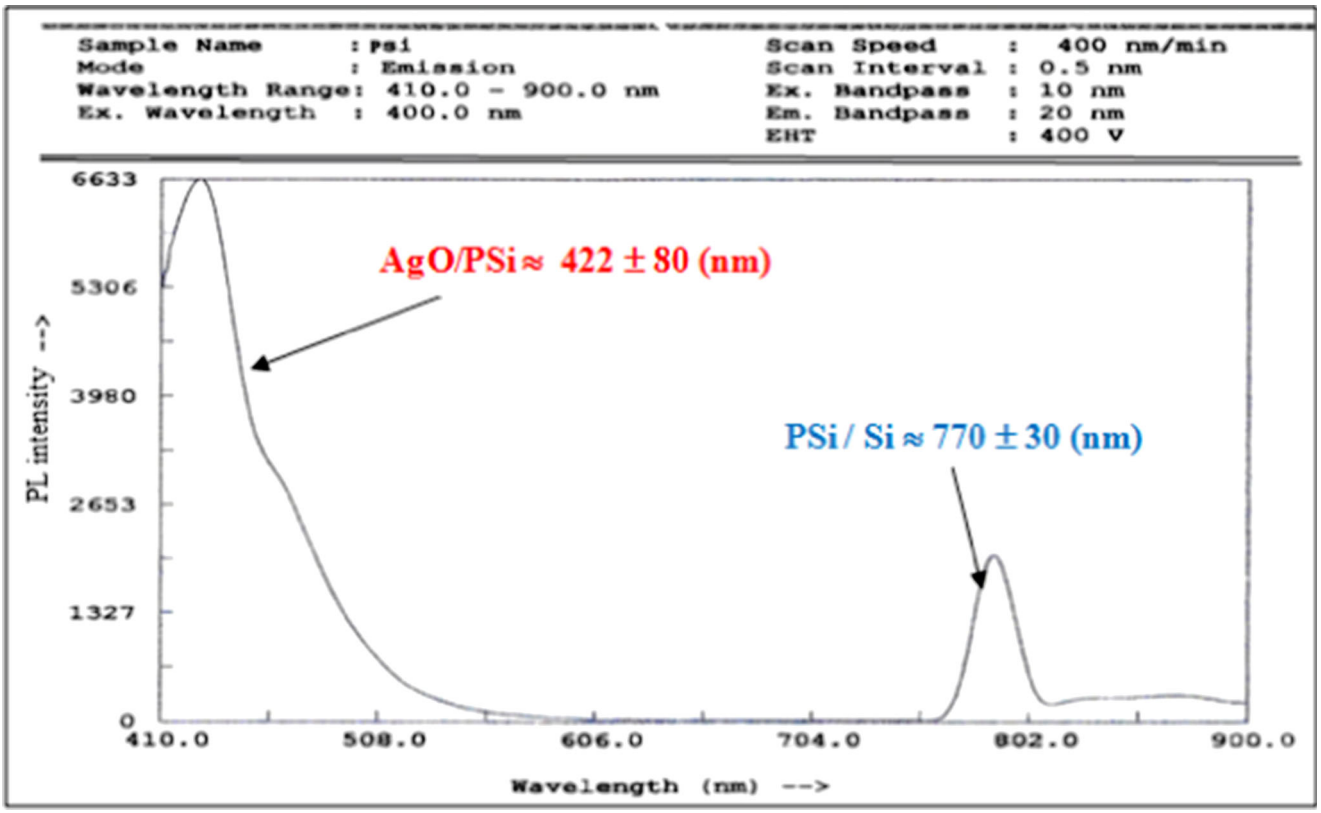

Fig. 7 Photoluminescence spectra of AgO heretojunction

and compared with the Joint Committee on Powder Diffraction Standards (JCPDS), silver file No. 04–0783. The XRD study confirms / indicates that the film is face center cubic (FCC) silver thin film [18]. The diffraction angles 64.57°, 77.51° were attributed for (200) and (111) AgO thin films. The crystallite size was calculated by using Debye-Scherrer's relation [19]:

$$G_s = \frac{0.9\lambda}{\beta \cos\theta} \tag{1}$$

where G_S is the crystallite size, β the full width at half maxima, θ is the angle of diffraction, and λ is the X-ray wavelength.

The strain η and the dislocation density δ values can be evaluated by using relations 2 and 3 below [19], see Table 1:

$$\eta = \beta \frac{\cos\theta}{4} \tag{2}$$

$$\delta = \frac{1}{G_S^2} \tag{3}$$

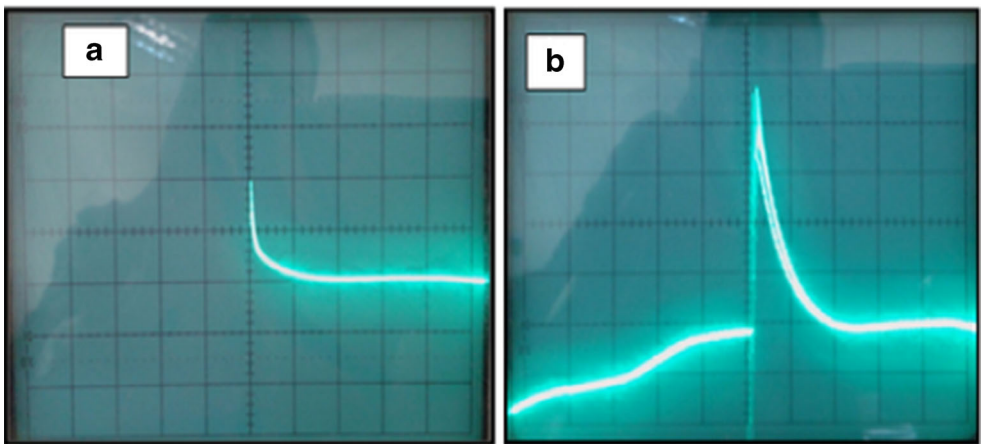

Fig. 8 Images for the Open-Circuit Voltage Decay Photograph for (**a**) PSi and (**b**) AgO/PSi/Si

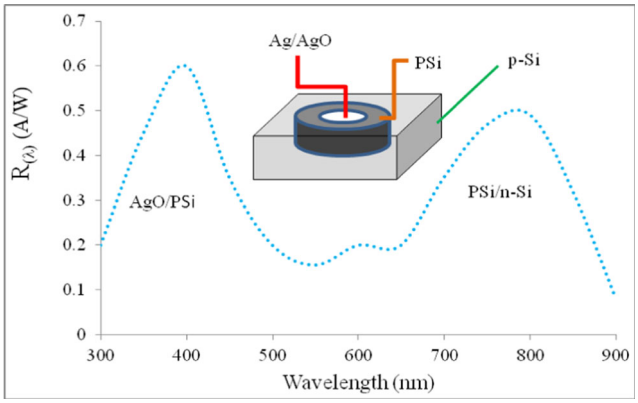

Fig. 9 Spectral responsivity curve of AgO/PSi/ Si

The crystallite size of AgO was greater than that of Ag but, the strain and dislocation density is smaller than it.

Figure 2 illustrated the scanning electron microscope images of the Ag and AgO thin films grown on glass substrates which consists of a uniform distribution of semi-spherical shaped of nanostructured grains with a diameter of about (2 μm). This structure peats throughout the materials with closely packed to each other indicating good adhesiveness of film with the substrate.

The optical band gap of the AgO thin film was calculated from the transmission and absorption spectra. Figure 3 displays the transmission as a function of wavelength. It is obvious that the film gives good transparency characteristics at the spectral range (400- 900) nm. Figure 4 shows the band gap of AgO thin films measured from the plot of $(\alpha h\upsilon)^2$ versus photon energy $h\upsilon$ (where α is the absorption coefficient). By extrapolating the linear part of the curve toward the photon energy axis, the band gaps of AgO thin films were found to be 2.2 eV and 3.2 eV. The existence of two energy gap could be attributed to the fluctuation of absorption edge which is due to the energy band structure and the variation of density of state with the energy level, also this variation can be attributed to the low thickness of the film.

The electrical resistivity of the prepared AgO thin film is sensitive to the growth of the phase and microstructure. The single phase of AgO films formed at 300 °C oxidation temperature and 60 min oxidation time exhibited the electrical resistivity and electrical mobility values which , were ($6.5x10^{-4}\Omega$.cm) and ($79cm^2$/V.s) respectively. The positive sign of the Hall coefficient obtained confirms the p-type conductivity of the AgO thin films, see Fig. 5.

Figure 6 reveals the (3-D) AFM images and the chart distribution of AgO thin film. AFM image proves that the grains were uniformly distributed within the scanning area (500× 500nm) with individual columnar grains extending upwards. The average grain size of pore was measured from AFM analysis using special software which was found to be around 32 nm depending on preparation conditions (current density of 10 mA/cm^2 and 15 min etching time).

Photoluminescence (PL) of AgO/PSi/n-Si film has been recorded by excitation the sample with laser wavelength of 400 nm. Figure 7 shows the PL spectrum of AgO deposited on porous silicon (PSi) substrate, a typical luminescence profile with two peaks was observed. Higher energy (shorter wavelength) excitation photons causes more photons to be emitted before luminescence occurs. If the excitation energy

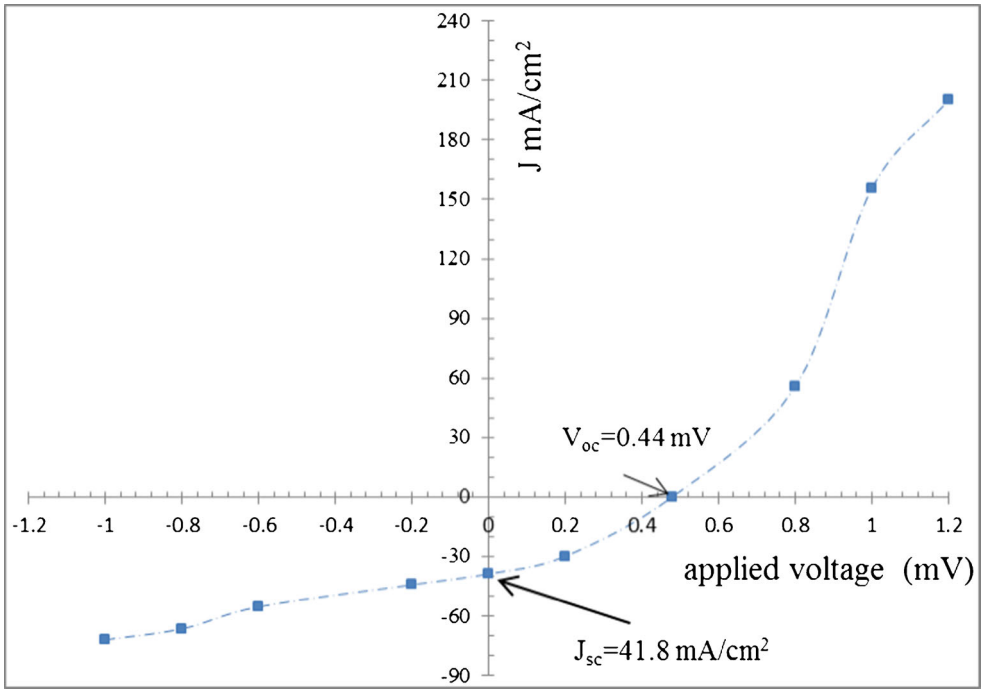

Fig. 10 I-V characteristics of Ag/AgO/n-PSi/Si photodetector

is less than the energy difference between the ground state and the first excited state, then no optical absorption will occur, resulting in no photoluminescence [20]. For pure AgO a strong PL band with a peak position centered at 2.85 eV (422 nm) was obtained which was less than the optical band gap of AgO film 3.70 eV and the second peak position was centered at 1.66 eV (770 nm). Therefore, the emission peak might correspond to the electron transition from the donor level formed by oxygen vacancy to the valance band. The electron in the donor level jumps to the valence band and the transition generates violet light emission .

Figure 8 shows that the PSi/Si have higher life time (133 μsec) at (15 mA/cm^2) etching current density, but the life time reach to (283 μsec) for 10 min etching time for AgO/PSi/Si which means that the probability of recombination will be decreased. Figure 9 reveals that the spectral responsivity curve(R_λ) of AgO/PSi/ Si which was consists of two peaks of response; the first peak was located at 400 nm due to the absorption edge of AgO/PSi nanoparticles , while the second peak was located at 770 nm due to absorption edge of silicon.

The improvement in responsivity of photodetectors after the deposition of AgO can be ascribed to the following reasons; (i) Increasing the depletion width, (ii) Minimization the surface defect states, (iii) Increasing the carrier collection efficiency and (iv) Increasing the light absorption.

Figure 10 shows the I-V characteristics for AgO/n-PSi/Si. The measured short-circuit current, open-circuit voltage, fill factor and efficiency are 2.9 μA, 0.44 mV, 46.96 % and 15.5 % respectively at flueunce of 40 μW/cm^2. All the results relieve that the sandwich structure AgO/n-PSi/Si could be used as a solar cell.

4 Conclusions

The p-AgO/PSi/n-Si heterojunction was successfully fabricated by using electrochemical etching of silicon and the deposition of Ag thin films by thermal evaporation and rapid oxidation at 300 °C. AgO show a good transparency in the spectral range (400- 900) nm and the electrical characteristics of heterojunction were strongly dependent on the structure. The porosity of Si has improved the performance of p-AgO/PSi/n-Si heterojunction to be very efficient materials for solar cell applications.

References

1. Fortin E, Weichman FL (1964) Photoconductivity in Ag_2O. Phys Stat Sol (B) 5:515–519
2. Wei W, Mao X, Ortiz LA, Sadoway DR (2011) Oriented silver oxide nanostructures synthesized through a template-free electrochemical route. J Mater Chem 21(2):432–438
3. Jobst PJ, Stenzel O, Schürmann M, Modsching N, Yulin S, Wilbrandt S, Gäbler D, Kaiser N, Tünnermann A (2013) Optical properties of unprotected and protected sputtered silver films: Surface morphology vs. UV/VIS reflectance. Adv Opt Technol 3:91–102
4. Vucina T, Boccas M, Araya C, Ahhee C (2006) Gemini's Protected Silver Coatings: first two years in operation. Proc SPIE 6273:62730W
5. Sheikh DA, Connell SJ, Dummer RS (2008) Durable silver coating for Kepler Space Telescope primary mirror. Proc SPIE 7010:70104E
6. Rehren C, Isaac G, Schlogl R, Ertl G (1991) Surface and subsurface products of the interaction of O_2 with Ag under catalytic conditions. Cat Lett 11(3):253–265
7. Sun Y (2010) Conversion of Ag nanowires to AgCl nanowires deco- rated with u nanoparticles and their photocatalytic activity. J Phys Chem 114(5):2127–2133
8. Lee U, Ham S, Han C, Jeon YJ, Myung N, Rajeshwar K (2010) Mild and facile synthesis of Ag_2S nanowire precursor using mercaptoacetic acid as a reductant/stabilizer and its subsequent conversion to Ag_2S or CdS nanowires. Mater Chem Phys 121(3):549–554
9. Garner WE, Reeves LW (1954) The thermal decomposition of silver oxide. Trans Faraday Soc 50:254–260
10. Muhsien MA, Hamdan HH (2012) Preparation and characterization of p- Ag_2O/n-Si heterojunction devices produced by rapid thermal oxidation. Energy Proc 18:300–311
11. Al-kuhaili MF (2007) Characterization of thin films produced by the thermal evaporation of silver oxide. J Phys D Appl Phys 40:2847–28
12. Petersson LAA, Snyder PG (1995) Preparation and characterization of oxidized silver thin films. Thin Solid Films 270:69–72
13. Raju NRC, Kumar KJ, Subrahmanyam A (2009) Physical properties of silver oxide thin films by pulsed laser deposition: effect of oxygen pressure during growth. Journal of Physics D 42(13):ID135411
14. Varkey AJ, Fort AF (1993) Some optical properties of AgO and Ag_2O films produced by chemical-bath deposition. Solar Energy Mater Solar Cells 29:253–259
15. Yuan Y, Yuan R, Chai Y, Zhuo Y, Mao L, Yuan S (2010) A novel label free electrochemical immune-sensor for carcino-embryonic antigen detection based on the [Ag–Ag_2O] / SiO_2 nano-composite material as a redox probe. J Electro - Anal Chem 643:15–19
16. Zhao KM, Liang Y, Gao XY, Chen C, Chen XM, Zhao XW (2012) Evolution of the structural and optical properties of silver oxide films with different stoichiometries. Chin Phys B 21:066101
17. Narayana Reddy P, Sreedhar A, Hari Prasad Reddy M, Uthanna S, Pierson JF (2011) The effect of oxygen partial pressure on physical properties of nanocrystalline silver oxide thin films deposited by RF magnetron sputtering. Cryst Res Technol 46:961–966
18. Lanje AS, Sharma SJ, Pode RB (2010) Synthesis of silver nanoparticles: a safer alternative to conventional antimicrobial and antibacterial agents? J Chem Pharm Res 2(3):478
19. Girija K, Thirumalairajan S, Mohan SM, Chandrasekaran J (2009) Structral, Morphological and optical studies of cdse thin films from ammonia bath. Chalocogenide Lett 68:351–357
20. Gangopadhyay P, Magudapathy P, Kesavamoorthy R, Panigrahi BK, Nair KGM, Satyam PV (2004) Growth of silver nanoclusters embedded in soda glass matrix. Chem Phys Lett 388:416